

Supporting Materials

Twist Angle-Dependent Work Functions of Twisted Bilayer Graphene

Shangzhi Gu^{1,2, #}, Wenyu Liu^{1, #}, Shuo Mi^{1, #}, Guoyu Xian², Jiangfeng Guo¹, Fei Pang¹, Shanshan Chen^{1, *}, Haitao Yang^{2, *}, Hongjun Gao², Zhihai Cheng^{1, *}

¹ *Beijing Key Laboratory of Optoelectronic Functional Materials & Micro-nano Devices,
Department of Physics, Renmin University of China, Beijing 100872, China*

² *Beijing National Laboratory for Condensed Matter Physics, Institute of Physics, Chinese
Academy of Sciences, P.O. Box 603, Beijing 100190, China*

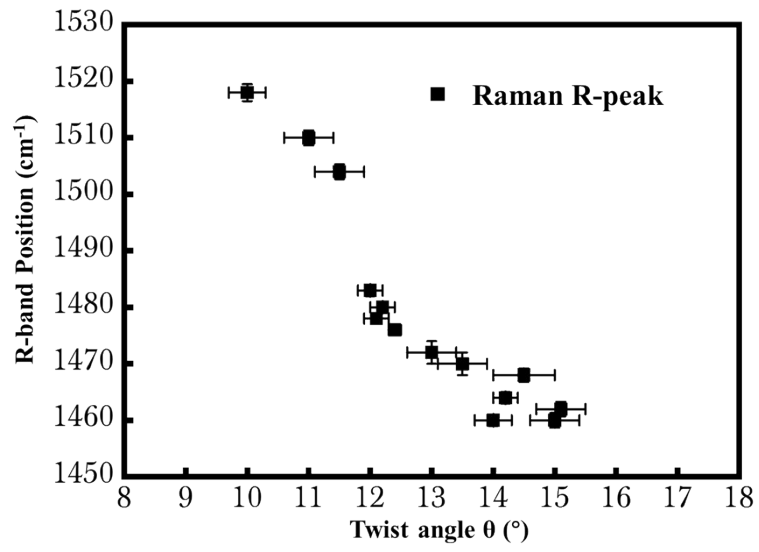


Figure S1. Dependence of the R-peak position on the twist angle for tBLG. The R-peak position decreased as the twist angle increased from 10° to 15° .

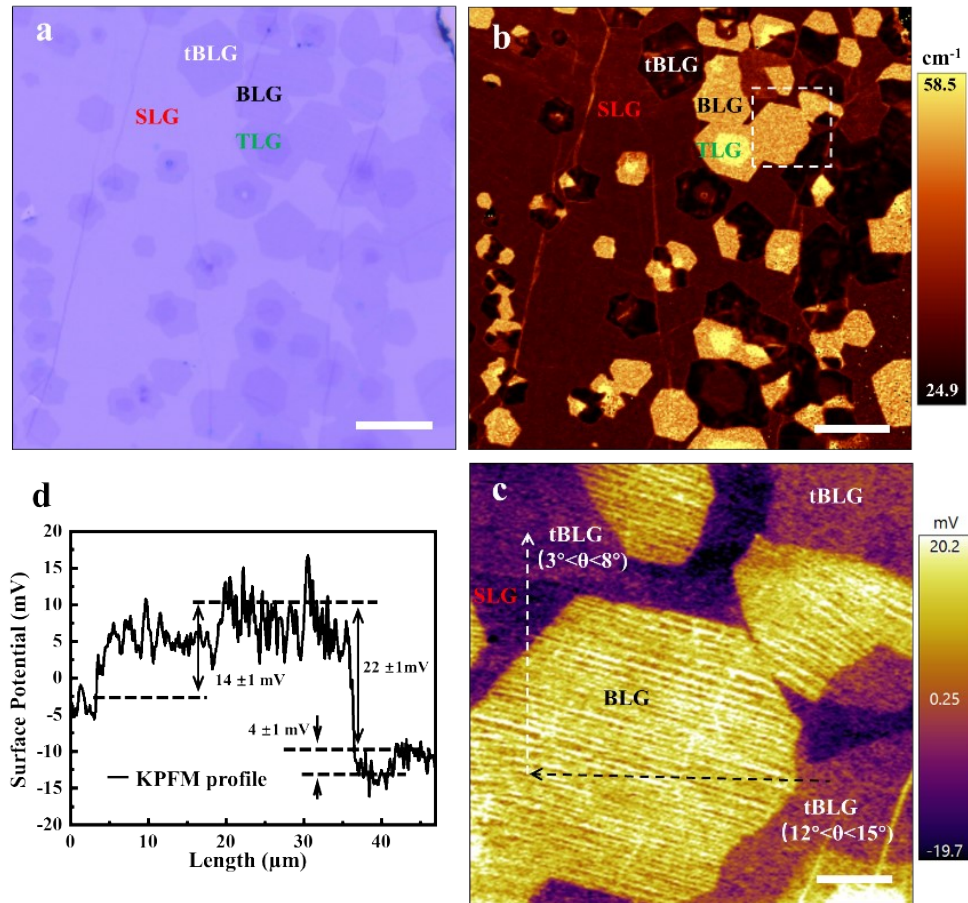


Figure S2. Optical images and Raman maps of the CVD-grown twisted multilayer graphene. (a) Optical image of CVD-grown multilayer graphene transferred onto the SiO₂/Si substrate, showing the continuous top graphene layer and the partial BLG (and TLG) in the bottom layer. (b) Corresponding Raman 2D-peak FWHM images of the area shown in (a). The SLG, BLG, tBLG, and TLG regions were clearly resolved. (c) Magnified KPFM image corresponding to the region indicated by the dashed white box in (b). These BLG regions consist of tBLG ($3^\circ < \theta < 8^\circ$) or tBLG ($12^\circ < \theta < 15^\circ$) and BLG domains. (d) Surface-potential line profile along the “black dashed line in the cross-sectional image of (c). Scale bar: (a, b) 30 μm ; (c) 6 μm .

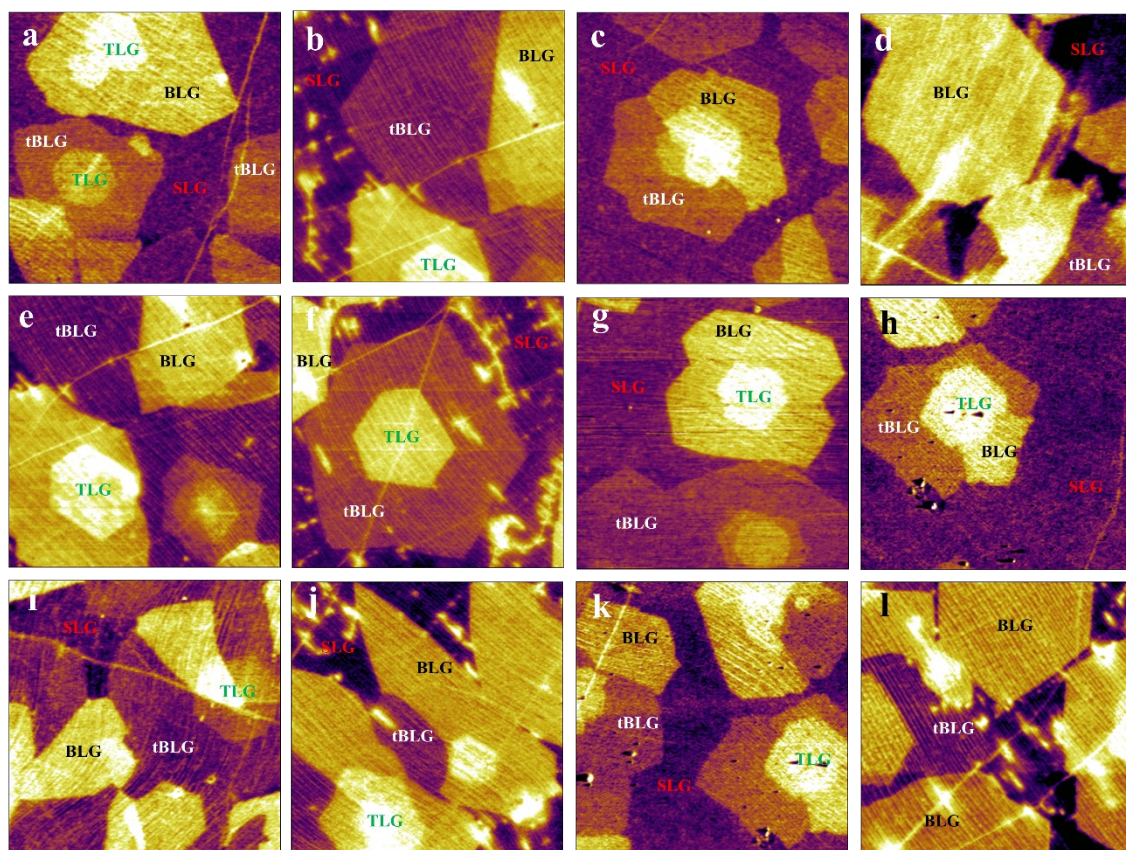


Figure S3. KPFM surface-potential images of twisted graphene layers with different interlayer twist angles (0° – 30°) and domain structures. The BLG, tBLG, and TLG domains of various irregular shapes were distinguished by their twist angle-dependent surface potentials. Image size: $30\ \mu\text{m} \times 30\ \mu\text{m}$.

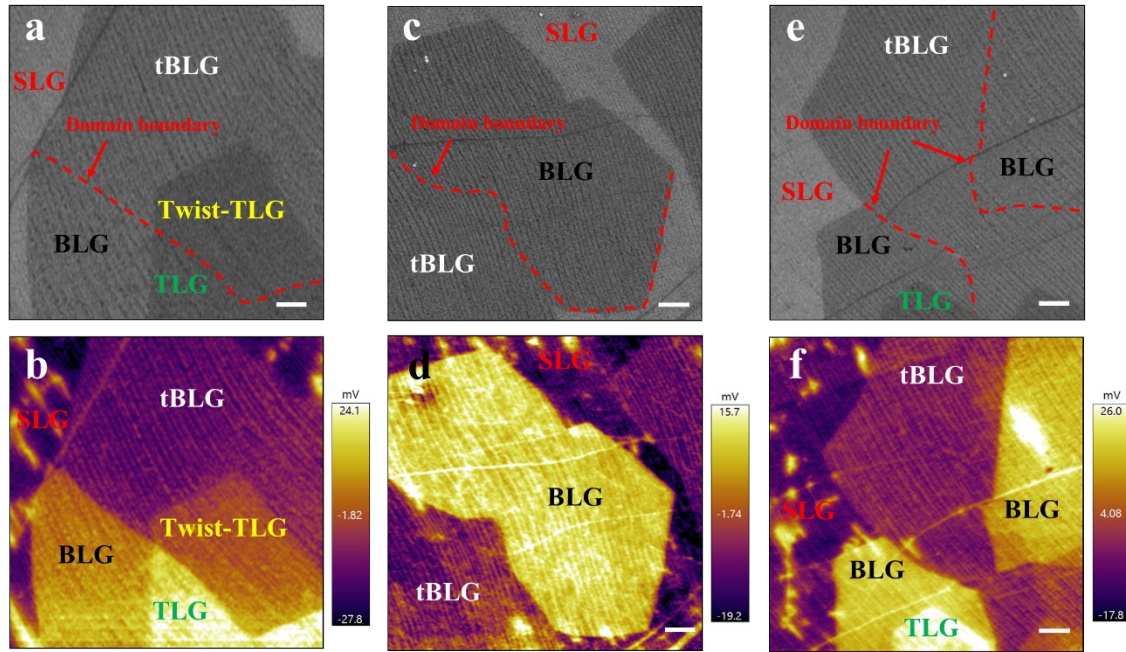


Figure S4. SEM images and KPFM mapping of twisted multilayer graphene. (a, c, e) SEM images of multilayer graphene films transferred onto the SiO_2/Si substrate. (b, d, f) KPFM images corresponding to (a), (c), and (e), respectively, in which the SLG, BLG, tBLG, TLG, and tTLG region are marked. The tBLG and BLG domains are clearly resolved in the KPFM surface-potential images but cannot be resolved in the SEM images, owing to their identical contrasts. The SLG, BLG, tBLG, TLG, and tTLG areas are also marked in the SEM images (a, c, e) according to the corresponding KPFM surface-potential images (b, d, f). The TLG and tTLG areas marked in (a) and (b) are worthy of further investigation. The strain-induced wrinkles within the graphene films are observed in both the SEM and KPFM images. The scale bar represents $6\ \mu\text{m}$ in all the images.

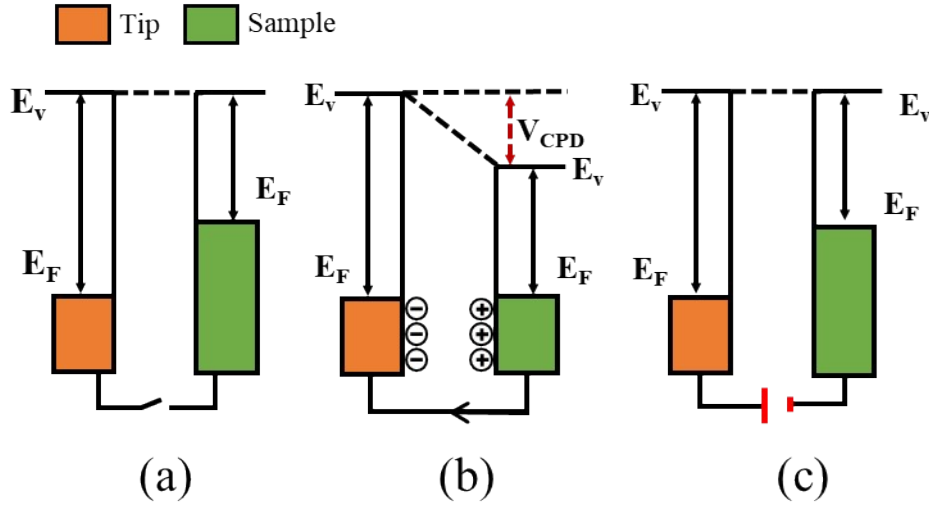


Figure S5. Electronic energy levels between the AFM tip and sample, illustrating the principle of the KPFM mode. (a) Tip and sample are separated with no electrical contact. They have equal E_v values but different E_F values. Here, E_v represents the vacuum energy level, E_F represents the Fermi energy level, and V_{CPD} represents the contact-potential difference. (b) Tip and sample are in electrical contact, with electron transfer from the sample with a higher E_F to the one with a lower E_F . (c) By applying a direct-current (DC) voltage V_{DC} ($V_{DC} = V_{CPD}$) between the tip and the sample, the vacuum level is realigned.

Generally, the work-function value indicates the strength of the electron binding in the metal. A larger value indicates that it is more difficult for electrons to leave the metal. The work function is usually expressed as the difference between the vacuum energy level and the Fermi level, which is given by the following formula: $W = E_0 - E_F$, where W represents the work function. Fig. S5 shows the principle of the potential difference between the tip and the sample. Fig. S5(a) presents the energy levels of the tip and sample surface when the tip and sample are not electrically connected. The vacuum levels are associated, but the Fermi levels are different. The tip and sample have different work functions, and $W_{tip} > W_{sample}$. When electrical conduction occurs between the tip and the sample, the surface charge is redistributed, resulting in alignment of the Fermi level. The system achieves an equilibrium state, as shown in Fig. S5(b). At this time, the tip and sample charge each other to produce different surface potentials, which is obvious when $\varphi_{tip} < \varphi_{sample}$, where φ represents the surface potential. The relationship between the work function and the surface potential can be expressed as follows:

$$W_{sample} - W_{tip} = -e(\varphi_{sample} - \varphi_{tip}).$$

If an external voltage with the same magnitude as V_{CPD} and the opposite sign is applied between the tip and the sample, the electrostatic force between the tip and the sample is eliminated, and the vacuum energy levels of both are readjusted. The data obtained via the KPFM measurement are the contact-potential differences (V_{CPD}) of the sample relative to the tip. The contact-potential difference is directly proportional to the work-function difference between the tip and the sample.

$$V_{CPD} = \varphi_{sample} - \varphi_{tip} = -(W_{sample} - W_{tip})/e$$

Therefore, we can directly obtain the work-function relationship using the surface-potential difference.